Rapid Communications

Forced wakes far from threshold: Stuart-Landau equation applied to experimental data

S. Boury,[1,2] B. Thiria,[3] R. Godoy-Diana,[3] G. Artana,[1] J. E. Wesfreid,[3] and J. D'Adamo[1,*]

[1]*Laboratorio de Fluidodinámica (LFD), Facultad de Ingeniería, Universidad de Buenos Aires (CONICET), Avenida Paseo Colón 850, C1063ACV, Buenos Aires, Argentina*

[2]*École Normale Supérieure de Lyon, 69007 Lyon, France*

[3]*Laboratoire de Physique et Mécanique des Milieux Hétérogènes (PMMH UMR 7636), CNRS, ESPCI Paris–PSL Research University, Sorbonne Université, Université Paris Diderot, 75005 Paris, France*

(Received 16 May 2018; published xxxxxx)

In this Rapid Communication, we study with the Stuart-Landau (SL) amplitude equation, a wake flow control scenario using experimental data from a cylinder wake forced by plasma actuators. Given the formal framework recently discussed by Gallaire *et al.* [Fluid Dyn. Res. **48**, 061401 (2016)] on pushing amplitude equations far from threshold, we analyze experimental data of a forced wake in order to test the SL reduced order model. Linear stability theory and global mode concepts are used to determine the SL parameters. The extension to forced wakes of the SL model had been proposed by Thira and Wesfreid [J. Fluid Mech. **579**, 137 (2007)] in the context of their study on stability properties, but its employment still remained an open question. Here, we show that a forced wake at a Reynolds number far from the first threshold can also attain the critical behavior described by the SL model.

DOI: 10.1103/PhysRevFluids.00.001900

Controlling wake flows presents many important applications in engineering and environmental sciences. The goals of control can be, for instance, the reduction of drag [1] or the modification of heat transfer on a structure subjected to an external flow [2]. Mechanically, the characteristic vortex shedding of wake flows is one of the cornerstones of many fluid-structure interaction problems, such as the vibration of bridge support cables or the thrust production mechanisms in animal locomotion. In active control strategies, considerable energy savings or engineering optimizations can be obtained through a careful choice of forcing parameters. In this Rapid Communication, we consider the canonical example of a circular cylinder, using an active control strategy based on the near-wall flow manipulation produced by plasma actuators [3]. The wake dynamics can be strongly affected when forcing the flow in the boundary layer around the cylinder.

Many studies on the subject of forced wakes have been conducted in the past 40 years using experimental, numerical, and theoretical approaches (see, e.g., Refs. [4–10]), and significant drag reductions have been associated with the stabilization of the Bénard–von Kármán instability (BvK) [6,9,11]. For wake flows with higher Reynolds numbers, or with less-energy-expensive actuators, comparable drag reductions have been attained through interfering with the formation of BvK structures by promoting symmetrical vorticity patterns [12,13].

The goal here is to examine a reduced model of the wake flow, the Stuart-Landau (SL) equation [14,15], in the case of a forced wake, identifying the parameters of the model with measurements from experiments. The application of the SL model to the unforced cylinder wake far from the

*jdadamo@fi.uba.ar

threshold of the BvK instability has been discussed recently [16]. Here, we show, using plasma-actuated wake experiments, that the forced wake can also be described in the same framework, exhibiting a critical behavior coupled to the forcing parameter.

It is well known that the Reynolds number $\mathrm{Re} = u_\infty d/\nu$ controls the transition from a stationary state in the wake to the BvK vortex shedding regime, where u_∞ is the flow velocity far away from the cylinder of diameter d and ν is the kinematic viscosity of the fluid. For the laminar regime in a two-dimensional (2D) flow, from $\mathrm{Re} \sim 5$, a recirculation region with two well-defined eddies of opposite circulation takes place, and therefore the streamwise central velocity u_x is negative in the near wake—we will consider hereafter a Cartesian (x, y) reference frame with the cylinder axis z perpendicular to the (x, y) plane and placed at its origin, and the flow far away from the cylinder moving in the positive x direction. At $\mathrm{Re}_c \simeq 47$ these eddies are no longer stable and the BvK instability sets in [4,17].

The wake dynamics close to the threshold can be modeled considering it as a propagating wave that grows from the origin, reaches a maximum, and decays afterwards. The spatial envelope of this coherent oscillation gives the amplitude of the so-called global mode (see, e.g., Refs. [18–20]), for which the dominant contribution is given by the first harmonic. The main flow structures, a double row of staggered vortices of opposite signs, are present for a large range of Reynolds numbers. The evolution of these structures and the supercritical transition near the stability threshold Re_c can be approximated with the complex Stuart-Landau (SL) equation (see, e.g., Refs. [4,21])

$$\tau \frac{da}{dt} = \epsilon(1 + ic_0)a - g(1 + ic_1)|a|^2 a, \tag{1}$$

where $a = \rho e^{i\phi}$ is a complex amplitude such that ρ is the amplitude of the global mode and ϕ the phase of the fluctuations, and τ, g, c_0, and c_1 are real coefficients. The Reynolds-dependent control parameter ϵ is a function of the distance to the critical Re_c value and can be written as $\epsilon = \mathrm{Re}^{-1} - \mathrm{Re}_c^{-1}$, as proposed by Ref. [22] and thoroughly discussed by Ref. [16]. The linear term in Eq. (1) characterizes the growth rate $\sigma_0 = \epsilon$ and the frequency $\omega_0 = \epsilon c_0$ of the fluctuations in the wake at the onset, while the saturating nonlinear term $\propto a^3$ is linked to the presence of a limit cycle due to the interaction between the zeroth, or stationary, mode that represents the time-mean flow and the first harmonic of the perturbation [22]. For the limit cycle regime, this model gives the evolution of the amplitude $\rho \sim \sqrt{\epsilon/g}$ and frequency shift $\tau\dot{\phi} \sim \epsilon(c_0 - c_1)$.

Concerning flow control, even though forced wakes lead to complex behaviors, they can be also modeled by the SL equation. Previous attempts can be found in Refs. [4,23,24] where a temporal forcing term $F \exp(2\pi i f_f t)$ is added to Eq. (1). However, in such models there is no link between the global mode dynamics and changes produced by the mean flow correction. On the other hand, it has been suggested [11] that the selected global modes in forced wakes could exhibit a similar critical behavior as that of free wakes near the threshold Re_c. Consequently, dynamic properties such as growth rate and frequency could be described by coupling the response amplitude a to a forcing-dependent parameter. A general case can be described considering a forcing with two parameters: an amplitude A and a frequency f_f; and the archetype of a cylinder forced by rotary oscillations has been discussed with numerical results by Ref. [25]. In such a forced cylinder wake, we also note a strong modification of the recirculation length behind the cylinder L_R, which corresponds to the streamwise location for which the streamwise time-mean flow $u_x = 0$ at $y = 0$ (see Fig. 1). If we consider the forcing as a mean flow perturbation that contributes to the zeroth harmonic of the wake, the following system for the established regime is obtained through a multiple-scale expansion [16,25],

$$\tau\dot{a} = \epsilon(1 + ic_0)a - g(1 + ic_1)|a|^2 a - \gamma(1 + i\beta)ab, \tag{2a}$$

$$b = F(|a|^2, A, f_f) = G(A, f_f) - H(A, f_f)|a|^2, \tag{2b}$$

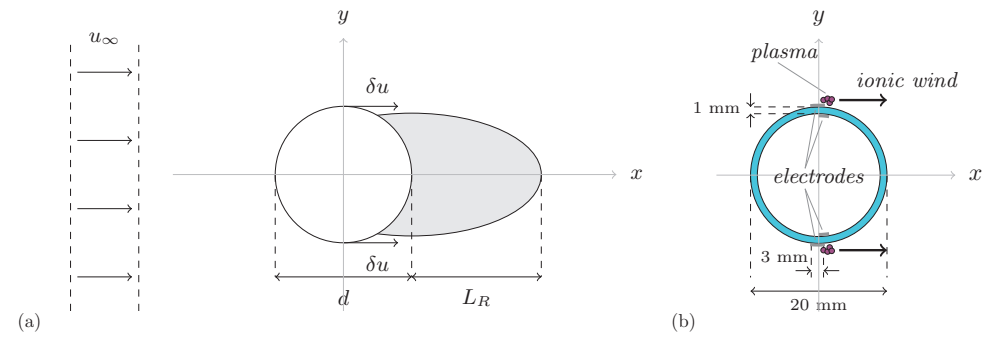

FIG. 1. Schematic diagrams of (a) a forced wake where the forcing is represented by a perturbation δu on the upper and lower parts of the cylinder that modifies the mean flow and so L_R. (b) Actual experimental setup, when forcing is obtained through plasma actuation.

where the dot stands for the time derivative, and γ and β are real coefficients. This leads us to define a forcing-dependent parameter b that can be represented either by the function $F(|a|^2, A, f_f)$ with A the forcing amplitude and f_f its frequency as suggested in Ref. [11], or by the pair of functions $G(A, f_f)$ and $H(A, f_f)$ as derived from the SL development. Therefore, the term $-\gamma(1 + i\beta)ab$ represents the coupling between the wake dynamics and the external forcing. Writing the complex amplitude $a = \rho e^{i\phi}$, Eq. (2a) leads to

$$\rho^2 = (\epsilon - \gamma b)/g = \hat{\epsilon}/g, \tag{3a}$$

$$\tau\dot{\phi} = \epsilon(c_0 - c_1) - \gamma b(\beta - c_1). \tag{3b}$$

The new control parameter $\hat{\epsilon}$ in Eq. (3b) governs the supercritical transition observed in the forced wake. The $\hat{\epsilon}$ parameter depends both on the Reynolds number (through ϵ, so that it can still describe the free wake transition) and the forcing term b. This means that stabilization can occur at a Re number other than the threshold without forcing Re_c.

While increasing the forcing amplitude A, the perturbation amplitude ρ, and accordingly $|a|^2$, might decrease. Thus, though we do not know the exact expression of the functions F, G, and H derived in (2b), there is strong evidence that $F(|a|^2, A, f_f) \to G(A, f_f)$ at high values of forcing, so that the parameter b only depends on the forcing properties A and f_f.

As mentioned above, the objective of the present Rapid Communication is to apply this theoretical framework to a realistic experimental case. For that purpose we use the experimental study of forced flow past a circular cylinder described in Ref. [26]. The setup, where plasma actuators are used to induce a ionic wind on the boundary layer of the cylinder, is represented schematically in Fig. 1. The cylinder of diameter $d = 0.02$ m is placed in an air flow of upstream velocity $u_\infty = 0.18$ m/s with viscosity $\nu = 1.5 \times 10^{-5}$ m^2/s, which gives a Reynolds number $\mathrm{Re} = 235$.

Forcing over the cylinder surface produces a strong coherent flow along the cylinder span which diminishes the possible spanwise variations due to three-dimensional instabilities or end effects [8,27,28]. Flow field measurements are performed using 2D particle image velocimetry (PIV) [29]. We refer the reader to D'Adamo *et al.* [26] for more details on the experimental setup. The experimental forcing parameter dc stands for duty cycle, a relationship between the time when the plasma is on, T_{ehd}, and the forcing time T_{burst} (see Ref. [29]). It is thus related with the actuator electric energy input (see Ref. [26]). As suggested in earlier studies, the modification of the flow transition could be forced by changing the actuation amplitude, its frequency, or both [11]. Here, it is the ionic wind amplitude of the plasma actuators that sets the amplitude of the forcing perturbation δu, showed schematically in Fig. 1. The forcing is stationary so it has no time dependence ($f_f = 0$) and, while we do not have a direct measurement of the velocity perturbation $\delta u \sim A$ added in

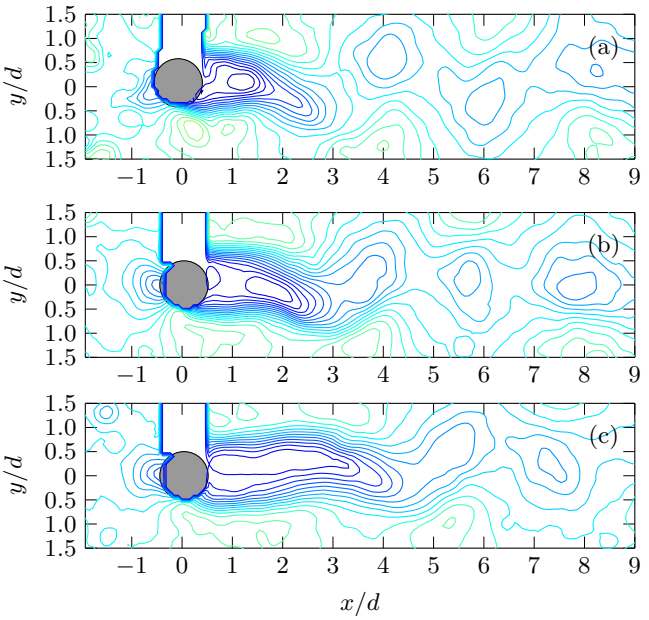

FIG. 2. Isocontours of the instantaneous 2D velocity modulus of the wake behind the cylinder for different duty cycles. (a) dc = 0 (no forcing), (b) dc = 10, (c) dc = 20. While increasing the forcing amplitude, an extension of the recirculation region length L_R, and an increase of the wavelength are observed.

the neighborhood of the cylinder wall (see Fig. 1), we know it is an increasing function of dc. We thus keep the nomenclature of the experimental setup forcing parameter dc in the following discussion.

Figure 2 shows typical wakes for different forcing amplitudes: dc = 0 (no forcing), dc = 10, and dc = 20. The velocity modulus $|\mathbf{u}| = (u_x^2 + u_y^2)^{1/2}$ is represented, where $\mathbf{u} = (u_x, u_y)$ is the velocity field measured experimentally. As we increase the forcing amplitude, we observe both a growth of the recirculation region and a stabilization of the wake, as vortex shedding takes place further downstream. Such changes are linked to the mean flow correction [8,30] and in this case they are introduced by the forcing. In order to examine the modification of the wake induced by the forcing, we explore now the evolution of the mean flow velocity. Figure 3(a) shows the evolution of the time-mean streamwise velocity $\langle u_x \rangle$ measured along the x axis at $y = 0$ as a function of the intensity of the plasma forcing dc. In the same graph, we observe that the mean velocity difference $\Delta u_{\min}$ between the natural wake and the forced one increases with dc, and it can be noticed that both the minimal value of $\langle u_x \rangle$ and its distance from the cylinder are modified. As dc increases, the mean flow correction has smaller variations so its global contribution to the zeroth harmonic is decreasing, which means that the wake tends to be stabilized. Now, the amplitude ρ of the SL-equation limit cycle can be estimated from intensity of the flow fluctuations. Following Ref. [30], we identify the order parameter ρ^2 from Eq. (3a) with the maximum of the transverse velocity fluctuations $\langle u_y'^2 \rangle^{1/2}$ along x at $y = 0$ [see Fig. 3(b)]. The position of this maximum changes with the strength of the forcing, as was also reported in Thiria and Wesfreid [25].

Let us recall the study of Zielinska *et al.* [19] on the mean flow modification of a wake in the supercritical regime. In their notation, when the flow is no longer stationary, the time-mean flow $\langle V \rangle = V_0 - \delta V$ results from a nonlinear correction δV to the stationary basic flow V_0. In the present case, the mean flow modifications represented by the quantity $\Delta u_{\min}$ are portrayed with respect to the nonlinear oscillations represented by ρ^2, as shown in Fig. 3(c). When the forcing is strong enough, $\Delta u_{\min} > 0.1$, ρ^2 depends linearly on the modifications of the mean flow $\Delta u_{\min}$. Thus,

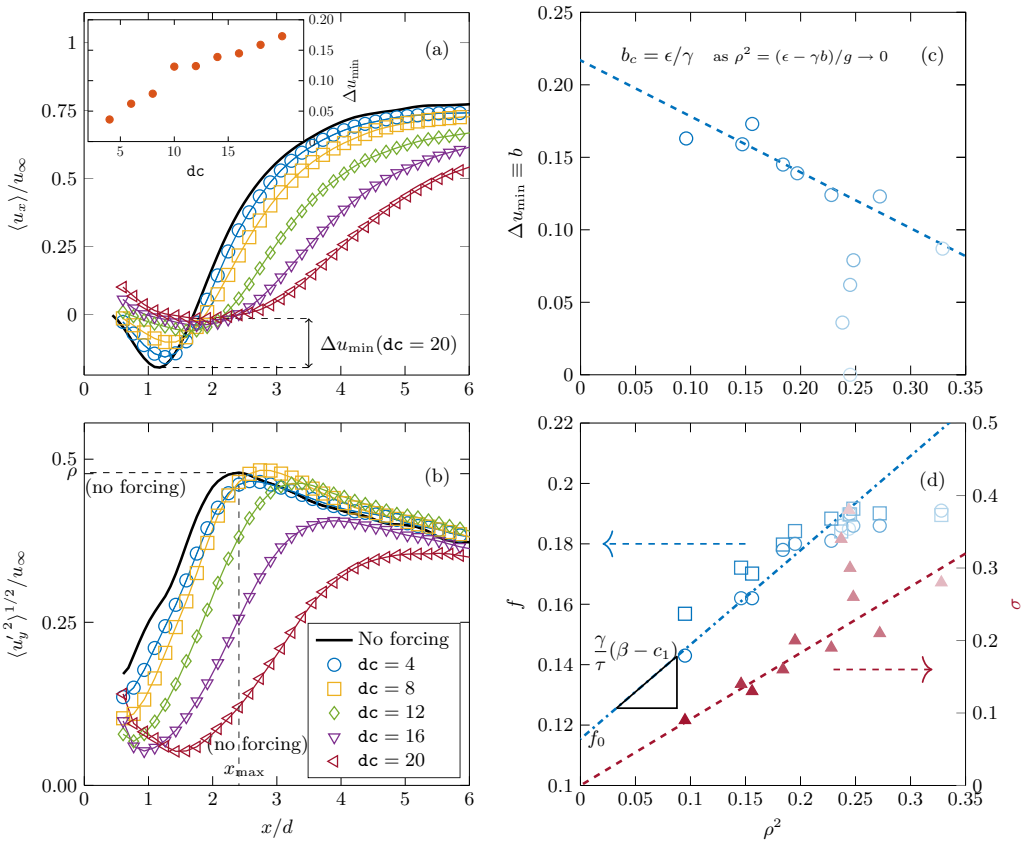

FIG. 3. (a) Evolution of the mean velocity measured along the x axis as a function of dc, where the different labels are displayed on (b). The definition of $\Delta u_{\min}$ is plotted in the case of $\mathtt{dc}=20$. The inset plot shows the values of $\Delta u_{\min}$ as a function of the forcing parameter dc. (b) Evolution of the spatial shapes of the global modes with the forcing dc. For each curve, its maximum defines a pair of values $(x_{\max},\rho)$. (c) Relationship between the squared amplitude ρ^2 and the characteristic modification of the mean flow given by $\Delta u_{\min}$. As $\Delta u_{\min}$ increases, ρ^2 tends to 0, corresponding to the wake stabilization. Linearity ceases to hold when the forcing weakens, which is displayed through a diminished color intensity of the plot markers. (d) Behavior of the selected frequency f of the global mode (◯ and □) and the growth rate σ (▲) as a function of the squared amplitude ρ^2; ◯ and ▲ are obtained through a linear stability analysis, and □ are determined from a Fourier decomposition of the experimental values. As $\rho^2\to 0$, the stable mean flow frequency $f_0\sim 0.115$. In the same sense, while increasing the forcing, the temporal growth rate decreases.

following Eq. (2a), we propose that the parameter for the mean flow correction b is equivalent to $\Delta u_{\min}$. The slope of the line displayed in Fig. 3(c) is therefore $-\gamma/g$.

To explore the stabilization of the wake, we perform a linear stability analysis based on the time-mean flow, as discussed by Refs. [31,32]. Following the methods provided for a local analysis by Ref. [33], we have access to the growth rate σ_0 and the frequency ω_0 of the selected unstable mode for each x-streamwise coordinate. The criterion for the prediction of global frequency for a spatially developing flow [34] is recalled in Appendix B. This predicted value is compared to a direct measurement through a Fourier decomposition of the experimental values $u_y(t)$ evaluated at a vicinity of $(x_{\max}, y=0, t)$. They are plotted in Fig. 3(d), showing that the linear stability analysis is accurate enough in our case. As we can see, the forced wakes tend to a stable stationary solution as the growth rate σ is a decreasing function of the nonlinear oscillations given by ρ^2. The behavior of the wake properties σ and f is very similar to the evolution observed for free wakes when

approaching the threshold of the instability by upper values of the Reynolds number ($\mathrm{Re} \to \mathrm{Re}_c^+$). It is noticeable in Eq. (3a) that when ρ^2 goes towards zero, which corresponds to $\hat{\epsilon} = 0$, we obtain a critical value $b_c = -\epsilon/\gamma$ that we can use to create a nondimensional transition parameter $(b_c - b)/b_c$. In the same sense, for small values of ρ, the frequency of the wake decreases through a linear dependence of slope $\gamma(\beta - c_1)/\tau$. Particularly, when $\rho^2 \to 0$, the forced wake frequency reaches a finite value identified as the stable flow frequency $f_0 \simeq 0.12$ [18,33], as in the nonforced scenario [see Fig. 3(d)]. The wave velocity $c = \lambda f$ is near constant ($c = 0.80 \pm 0.05$). The reduced parameter $(b_c - b)/b_c$ is therefore relevant to describe the forced wake transition at a fixed Reynolds number Re, and the parameter $\hat{\epsilon}$ would be a good choice to fully describe the Reynolds-dependent and forcing-dependent transition that leads to the BvK instability when we work in flow control.

Summarizing, we found strong evidence of a critical behavior of the mean flow parameter $b \to b_c$ at the transition to the flow stabilization. Consequently, the mean flow correction produced by the control is found to be a parameter for the bifurcation in the way defined in Eq. (2). The estimated Strouhal number $\mathrm{St} = f d/u_\infty$ corresponding to the value $b = b_c$ was $\mathrm{St} \simeq 0.12$, which is only slightly below the critical frequency selected at $\mathrm{Re} = \mathrm{Re}_c$.

Scaling laws based on the mean flow modification seem to remarkably describe and characterize the critical dynamics close to threshold under forcing conditions when flow control is performed with plasma actuators. Even more, the mean flow, which is a function of the forcing parameter (A, f_f) and the Reynolds number, does not involve directly the specific form of the external perturbation, but its consequence on average. The scenario should thus be similar with other forms of control such as body rotatory oscillations (see Ref. [35]).

The link between the mean flow correction $\Delta u_{\min}$ and the transition in the forced wake being established, we believe that this parameter, which is closely linked to the stabilization mechanisms, should be robust enough to describe critical behaviors in wake flows for a large range of forcing parameters and far from the critical Reynolds number. As a final note, we recall that, as the forcing also modifies the recirculation length scale L_R, a transition diagram between stable and unstable flow had been suggested in the $(\mathrm{Re}; L_R)$ plane (see Fig. 24 in Ref. [11]). The behavior of the recirculation length, both for the stable state and the vortex shedding, could be explained as a linear and nonlinear modification of the mean flow [19,30]. Therefore, we can relate it to the perturbation induced by the forcing and help to complete a transition diagram.

In this Rapid Communication, we expose that is possible to explain and predict the effect of an actuator on unstable flows. The steps described here offer a physical explanation of flow control mechanisms that go beyond a purely phenomenological description.

We acknowledge support from CONICET (Argentina) and CNRS (France) through the LIA PMF-FMF (Franco-Argentinian International Associated Laboratory in the Physics and Mechanics of Fluids).

APPENDIX A: STUART-LANDAU EQUATION WITH A FORCED TERM

We develop the equation corresponding to the forcing cases from the basis of the Stuart-Landau equation applied in wake flows by Refs. [16,22],

$$\frac{dA}{dT} = \lambda A - \mu |A|^2 A, \tag{A1a}$$

$$\lambda = \lambda_0 + \delta\lambda(F), \tag{A1b}$$

$$\mu = \mu_0 + \delta\mu(F), \tag{A1c}$$

where λ_0 and μ_0 are the coefficients when there is no forcing and $\delta\lambda(F)$ and $\delta\mu(F)$ are functions that depends on forcing. Therefore, Eq. (A1a) can be rewritten as

$$\frac{dA}{dT} = \lambda_0 A - \mu_0 |A|^2 A + \beta B A, \tag{A2a}$$

$$0 = -\beta B + f(|A|^2, F), \tag{A2b}$$

$$f(|A|^2, F) = \delta\lambda(F) - \delta\mu(F)|A|^2, \tag{A2c}$$

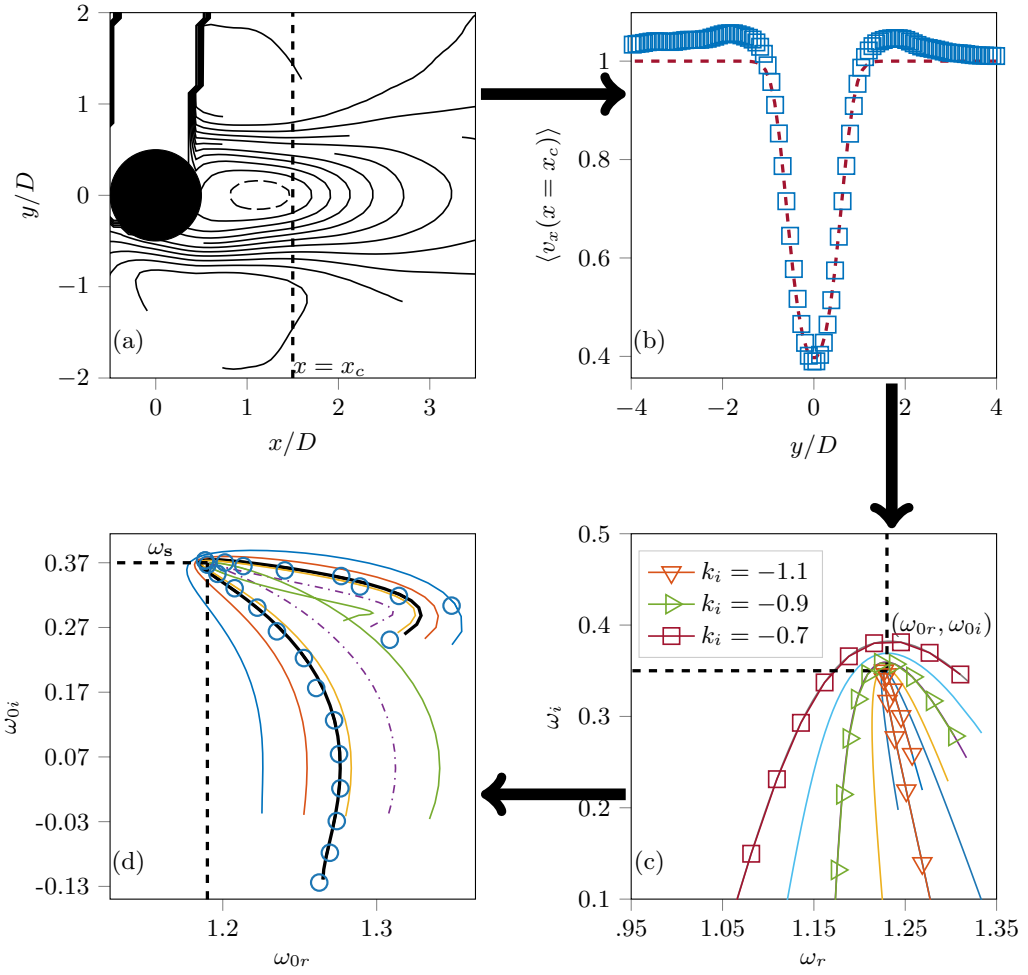

FIG. 4. Schematic representation of the necessary steps involved in the linear stability analysis: (a) Mean flow streamwise velocity contours, with a slight loss of symmetry is due to forcing, where a cut a $x = x_c$ gives (b) a mean velocity profile (square symbols) $\langle v_x(y, x = x_c)\rangle$, which is fitted by a function (dashed line) $u(y) = 1 - a_0 + a_0 \tanh[a_1(y/d)^2 - a_2)]$, where a_0, a_1, and a_2 are fitting parameters. Solving the corresponding dispersion relation, the Rayleigh equation for this inviscid instability, for a range of wave numbers $k = k_r + ik_i$, we obtain (c) a map for $k_i = \text{const}$ in the ω plane. At a critical point, a cusp on the $k_i = -0.7$ curve, the point $(\omega_{0r}, \omega_{0i})$ is determined for x_c. In (d) the results for each x position($\circ$ marks) are plotted in a ω plane. Criteria for the prediction of a global frequency in a spatially developing flow is given by the condition $\partial\omega/\partial x|_{x=x_s} = 0$ [34]. The saddle point $\omega_s = \omega(x = x_s)$ is obtained through an analytic continuation to complex values of $x = x_r + ix_i$ by inspecting the when a cusp point takes place (point-dashed curve) [36]. Considering all the cases, the points $\omega_s = (\omega, \sigma)$ provide the data for Fig. 3(d).

which is a particular case for Eq. (2), corresponding to the stationary evolution of B. A possible modification for an harmonic forcing is to consider $f(|A|^2, F)e^{i\omega_F t}$, as proposed by Ref. [11].

APPENDIX B: PREDICTION OF THE GLOBAL MODE FREQUENCY

The criterion proposed by Ref. [34] and applied to a wake flow in Refs. [36,37] for the prediction of global frequency for a spatially developing flow consists in finding a saddle point $\partial\omega_0/\partial x\|_{x=x_s} = 0$ of the complex function $\omega_0(x)$ through use of the Cauchy-Riemann equations and analytic continuation to complex values of $x = x_r + ix_i$. The procedure, applied as in other works [11,38] to the time-mean flow, is full summarized in Fig. 4. Hence, we could select the onset frequency $f = \omega_0(x_s)/2\pi$ for this spatially developing flow.

[1] H. Choi, W.-P. Jeon, and J. Kim, Control of flow over a bluff body, Annu. Rev. Fluid Mech. **40**, 113 (2008).

[2] J.-C. Lecordier, L. Hamma, and P. Paranthoen, The control of vortex shedding behind heated circular cylinders at low Reynolds numbers, Exp. Fluids **10**, 224 (1991).

[3] E. Moreau, Airflow control by non-thermal plasma actuators, J. Phys. D **40**, 605 (2007).

[4] M. Provansal, C. Mathis, and L. Boyer, Bénard–von Kármán instability: Transient and forced regimes, J. Fluid Mech. **182**, 1 (1987).

[5] S. Taneda, Visual observations of flow past a circular-cylinder performing a rotatory oscillation, J. Phys. Soc. Jpn. **45**, 1038 (1978).

[6] P. T. Tokumaru and P. E. Dimotakis, Rotary oscillation control of a cylinder wake, J. Fluid Mech. **224**, 77 (1991).

[7] H. Blackburn, F. Marques, and J. M. Lopez, Symmetry breaking of two-dimensional time-periodic wakes, J. Fluid Mech. **522**, 395 (2005).

[8] B. Thiria, S. Goujon-Durand, and J. E. Wesfreid, Wake of a cylinder performing rotary oscillations, J. Fluid Mech. **560**, 123 (2006).

[9] M. Bergmann, L. Cordier, and J. P. Brancher, Optimal rotary control of the cylinder wake using proper orthogonal decomposition reduced-order model, Phys. Fluids **17**, 097101 (2005).

[10] G. Tadmor, O. Lehmann, B. R. Noack, and M. Morzyński, Mean field representation of the natural and actuated cylinder wake, Phys. Fluids **22**, 034102 (2010).

[11] B. Thiria and J. E. Wesfreid, Stability properties of forced wakes, J. Fluid Mech. **579**, 137 (2007).

[12] T. N. Jukes and K. S. Choi, Long Lasting Modifications to Vortex Shedding Using a Short Plasma Excitation, Phys. Rev. Lett. **102**, 254501 (2009).

[13] J. D'Adamo, L. Leonardo, F. Castro, R. Sosa, T. Duriez, and G. Artana, Circular cylinder drag reduction by three-electrode plasma symmetric forcing, J. Fluids Eng. **139**, 061202 (2017).

[14] J. T. Stuart, On the non-linear mechanics of hydrodynamic stability, J. Fluid Mech. **4**, 1 (1958).

[15] L. D. Landau and E. M. Lifshitz, *Fluid Mechanics*, 1st Russian ed. (Nauka, Moscow, 1944).

[16] F. Gallaire, E. Boujo, V. Mantic-Lugo, C. Arratia, B. Thiria, and P. Meliga, Pushing amplitude equations far from threshold: Application to the supercritical Hopf bifurcation in the cylinder wake, Fluid Dyn. Res. **48**, 061401 (2016).

[17] C. P. Jackson, A finite-element study of the onset of vortex shedding in flow past variously shaped bodies, J. Fluid Mech. **182**, 23 (1987).

[18] J. E. Wesfreid, S. Goujon Durand, and B. Zielinska, Global mode behavior of the streamwise velocity in wakes, J. Phys. II **6**, 1343 (1996).

[19] B. J. A. Zielinska, S. Goujon-Durand, J. Dusek, and J. E. Wesfreid, Strongly Nonlinear Effect in Unstable Wakes, Phys. Rev. Lett. **79**, 3893 (1997).

[20] J. M. Chomaz, Global instabilities in spatially developing flows: Non-normality and nonlinearity, Annu. Rev. Fluid Mech. **37**, 357 (2005).

[21] C. Mathis, M. Provansal, and L. Boyer, The Bénard–von Kármán instability: An experimental study near the threshold, J. Phys. Lett. **45**, 483 (1984).
[22] D. Sipp and A. Lebedev, Global stability of base and mean flows: A general approach and its applications to cylinder and open cavity flows, J. Fluid Mech. **593**, 333 (2007).
[23] M. C. Thompson and P. Le Gal, The Stuart–Landau model applied to wake transition revisited, Eur. J. Mechan. B/Fluids **23**, 219 (2004).
[24] D. Olinger, A low-dimensional model for chaos in open fluid flows, Phys. Fluids A **5**, 1947 (1993).
[25] B. Thiria and J. E. Wesfreid, Physics of temporal forcing in wakes, J. Fluid Struct. **25**, 654 (2009).
[26] J. D'Adamo, L. M. Gonzalez, A. Gronskis, and G. Artana, The scenario of two-dimensional instabilities of the cylinder wake under electrohydrodynamic forcing: A linear stability analysis, Fluid Dyn. Res. **44**, 055501 (2012).
[27] P. Poncet, Topological aspects of three-dimensional wakes behind rotary oscillating cylinders, J. Fluid Mech. **517**, 27 (2004).
[28] N. Benard and E. Moreau, Response of a circular cylinder wake to a symmetric actuation by non-thermal plasma discharges, Exp. Fluids **54**, 1 (2013).
[29] The PIV field of view is normal to the cylinder, which has an aspect ratio of $L_z/D = 25.5$, and it has been taken at midspan ($z = 0$). The cylinder tips are free and wall mounted, respectively. We remark that the time lapse between the two frames of each image pair used for PIV was set to $\Delta t = 125$ ms and sets of 400 snapshots give a frequency resolution of $\Delta f = 0.04$ Hz or, in nondimensional units, $\Delta f d/u_\infty = 4 \times 10^{-3}$. The vortex shedding frequency, the plasma frequency, and the burst modulation of the plasma are respectively $f_{\rm shed} \simeq 1.5$, $f_{\rm ehd} = 5.6$ kHz, and $f_{\rm burst} = 200$ Hz. Hence, $T_{\rm burst} \ll T_{\rm shed}$, the flow is not altered by plasma modulation, and the forcing can be considered stationary. We performed this modulation in order to obtain a low-velocity ionic wind, and to smoothly change its intensity.
[30] B. J. Zielinska and J. E. Wesfreid, On the spatial structure of global modes in wake flow, Phys. Fluids **7**, 1418 (1995).
[31] D. Barkley, Linear analysis of the cylinder wake mean flow, Europhys. Lett. **75**, 750 (2006).
[32] S. Mittal, Global linear stability analysis of time-averaged flows, Int. J. Numer. Methods Fluids **58**, 111 (2008).
[33] G. Triantafyllou, M. Triantafyllou, and C. Chryssostomidis, On the formation of vortex streets behind stationary cylinders, J. Fluid Mech. **170**, 461 (1986).
[34] J. M. Chomaz, P. Huerre, and L. G. Redekopp, A frequency selection criterion in spatially developing flows, Stud. Appl. Math. **84**, 119 (1991).
[35] B. Thiria, G. Bouchet, and J. E. Wesfreid (unpublished).
[36] D. A. Hammond and L. G. Redekopp, Global dynamics of symmetric and asymmetric wakes, J. Fluid Mech. **331**, 231 (1997).
[37] B. Pier, On the frequency selection of finite-amplitude vortex shedding in the cylinder wake, J. Fluid Mech. **458**, 407 (2002).
[38] M. Khor, J. Sheridan, M. C. Thompson, and K. Hourigan, Global frequency selection in the observed time-mean wakes of circular cylinders, J. Fluid Mech. **601**, 425 (2008).